

See discussions, stats, and author profiles for this publication at: <https://www.researchgate.net/publication/280306746>

Task-Oriented Grasp Planning Based on Disturbance Distribution

Conference Paper · January 2013

DOI: 10.1007/978-3-319-28872-7_33

CITATIONS

7

READS

141

2 authors, including:



Yun Lin

University of South Florida

12 PUBLICATIONS 93 CITATIONS

SEE PROFILE

Task-Oriented Grasp Planning Based on Disturbance Distribution

Yun Lin and Yu Sun

Abstract One difficulty of task-oriented grasp planning is task modeling. In this paper, a manipulation task was modeled by building a non-parametric statistical distribution model from disturbance data captured during demonstrations. This paper proposes a task-oriented grasp quality criterion based on distribution of task disturbance and uses the criterion to search for a grasp that covers the most significant part of the disturbance distribution. To reduce the computational complexity of the search in a high-dimensional robotic hand configuration space, as well as to avoid a correspondence problem, the candidate grasps are computed from a reduced configuration space that is confined by a set of given thumb placements and thumb directions. The proposed approach has been validated with a Barrett hand and a Shadow hand on several objects in simulation. The resulting grasps in the evaluation generated by our approach increase the coverage of frequently-occurring disturbance rather than the coverage of a large area with a scattered distribution.

1 Introduction

Manipulation and grasp have been active research topics in robotics. One of the primary goals of the research is the choice of an appropriate grasp, in terms of task requirement and stability properties, given an object associated with a manipulation task to be performed [1]. Such a problem is referred to as the grasp synthesis problem. To solve this problem, different approaches and algorithms have been developed for the robotic hand to execute a stable manipulation task.

Yun Lin

University of South Florida, 4202 E. Fowler Ave., ENB118, Tampa, FL 33620-5399, e-mail: yunlin@mail.usf.edu

Yu Sun

University of South Florida, 4202 E. Fowler Ave., ENB118, Tampa, FL 33620-5399, e-mail: yusun@cse.usf.edu

One solution to grasp synthesis problem is grasp planning. Grasp planning uses optimization mathematics to search for the optimal contact placement on an object, which gives rise to difficulty in choosing a quality criterion for the optimization procedure. One widely-used quality criterion is the force-closure property, which measures the capability of a grasp to apply appropriate forces on an object to resist disturbances in any direction, defined as the radius of the largest six-dimensional wrench space sphere centered at the origin and enclosed with the unit grasp wrench space [2]. Related research was developed in [3, 4, 5, 6], etc. Nevertheless, they are task-independent, in which an evenly distributed disturbance in all directions is assumed.

In many manipulation tasks, however, such as drinking, writing and handling a screwdriver, a task-related grasp criterion has to be applied for the choice of appropriate grasp configurations for different task requirements. A typical task-oriented grasp method is to choose a suitable task wrench space (TWS) and then measure how good a task wrench space can be fitted into a grasp wrench space [4, 7, 8, 9, 10]. Few works have considered the task information in grasp planning due to the difficulty of modeling a task [7, 9, 11]. To obtain the task wrench space in reality, necessary sensors are required to measure the contact regions and contact normals, which remains a challenge. This is the main reason why most works empirically approximate the task wrench space rather than actually measure it. Instead of a wrench space ball used in force-closure quality measure, Li and Sastry [7] developed a quality criterion to measure the ability of a grasp to perform a task wrench space using a six-dimensional wrench space ellipsoid to better approximate a task. The research in [10] approximated the task wrench space as a task polytope and focused on the computation of task-oriented quality measures.

Pollard [4] proposed the object wrench space (OWS) that takes the complete object geometry into consideration. The OWS integrates all disturbance wrenches that can be exerted anywhere on the object. Borst et al. [9] presented an algorithm to approximate the OWS by an ellipsoid and to measure how good the OWS ellipsoid can be fitted into a Grasp Wrench Space (GWS). The idea of OWS takes all possible disturbances into account, which is good for unknown tasks but is not task-specific; for a specific task, a grasp does not need to perform the whole OWS but to perform the required subset TWS of the task wrench space.

Another difficulty of task-oriented grasp planning is the computational complexity of the searching in the high-dimensional hand configuration space. It is, therefore, natural to introduce human experience relative to a task [12, 13, 14, 15, 16, 17]. Aleotti and Caselli [18] used data gloves to map human-hand to robotic-hand workspace and captured the task wrench space in virtual reality. They also considered a database of candidate grasps, and grasps were evaluated by a task-related quality measure. However, the correspondence problem has been a crucial issue to map between different configuration spaces of the human hand and the robotic hand. Research in [19] searched for candidate grasps by a shape-matching algorithm and evaluated the grasps by a task-oriented criterion. However, the same modeling problem of the TWS still exists and the work also relies on empirical modeling.

This paper proposes a grasp quality criterion, called the task coverage grasp quality metric, to compute the proportion of task disturbance that a grasp covers. Instead of assuming an evenly-distributed task wrench space, this approach takes into account the task disturbance distribution measured from human demonstration, since it is possible that disturbance wrenches in some directions occur more frequently than in other areas, even if they may be smaller than wrenches that occur less frequently. In two tool manipulations, for example, a knife and a fork have similar shapes but have disturbance wrench distribution along different directions, hence favoring different grasps. Therefore, a targeted grasp is prone to increasing the coverage of most frequent disturbances, rather than a grasp with the same coverage of the area with scattered distributed disturbance. To reduce the computational complexity of the search in high-dimensional robotic hand configuration space, as well as to avoid a correspondence problem, the candidate grasp is computed from a set of given thumb placements rather than contact points ([20, 21, 22, 23, 24]) on an object surface. One advantage of thumb placement is that it is independent of the physical constraints of a given hand, which has the problem of solving the inverse kinematics that satisfies the constraints imposed by contact points [25]. Every thumb placement is associated with the direction thumb should point to, which further reduce the search space of wrist positions and orientations.

2 Grasp Analysis

2.1 Grasp Preliminaries

Considering a multi-fingered robotic hand grasping an object, a grasp comprises multiple contact points. Assuming a hard finger model of the grasp [26], i.e., point contact with friction (PCWF), the most common friction model is Coulomb's friction model; at each local contact, the tangential force is bounded by the normal force, $f^t \leq \mu f^n$, where f^t is the tangential force component, f^n is the normal force component, and μ is the coefficient of friction. Thus, all feasible contact forces are constrained to the friction cone. The friction has a vertex at the contact point, and the axis is along the contact normal, with an opening angle of $2\tan^{-1}\mu$. For the convenience of computation, the circular friction cone is usually approximated with an m -sided pyramid. Then, any contact force f_i at the i^{th} contact that is within the constraint of friction cone can be represented as a convex combination of the m force vectors on the boundary of the cone:

$$f_i \approx \sum_{j=1}^m \alpha_j f_{ij} \quad (1)$$

where coefficient $\alpha_j \geq 0$, and $\sum_{j=1}^m \alpha_j = 1$.

The 3-d force vector f_i and torque vector τ_i can be written as a wrench w_i . Each contact can be described with a six-dimensional vector of wrench w_i :

$$w_i = \begin{bmatrix} f_i \\ \tau_i = \lambda(d_i \times f_i) \end{bmatrix} \quad (2)$$

where d_i is the vector from global origin of the object to the contact point and λ is the scale factor of torque to force conversion. λ can be set to be the inverse of the maximum radius from the torque origin so that torque is independent of the object scale [4].

Given n contact points of a grasp, the unit GWS, written as $W(G)$, can be defined as the linear combination of the unit wrench space at each contact:

$$W(G) = \{w | w = \sum_{i=1}^{mn} \alpha_i w_i, \alpha_i \geq 0, \sum_{i=1}^{mn} \alpha_i = 1, |w_i| = 1\} \quad (3)$$

In other words, UGWS is the set of all possible resultant wrenches that can be applied to the object by all the contacts if applying unit magnitude of contact force, i.e., the convex hull of the contact wrenches (Figure 1).

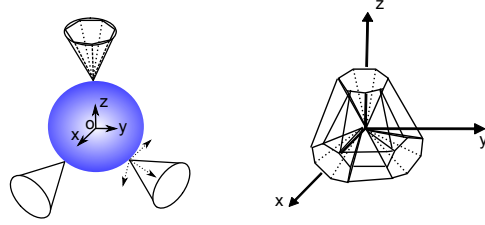


Fig. 1 The wrench space of a grasp.

A typical way of evaluating grasp quality is to compute force-closure, i.e., the ability of a grasp to equilibrate external force and moment in any directions by applying appropriate forces. It implies that if the origin of the wrench space is in the convex hull, then the grasp is force closure. Similar to the grasp wrench space, a task can also be described as the space of disturbance wrenches that must be applied to the object. Ferrari and Canny [3] quantified the force-closure property by the magnitude of the contact wrenches that can compensate the disturbance wrench in the worst case. If no task-oriented information is provided to form a subset of the whole space of wrenches, a typical task wrench space is a 6D ball T_{ball} centered at the wrench space origin, where external disturbance is uniformly weighted (Left of Figure 2). The grasp quality is the reciprocal of the scale to enlarge the grasp wrench space so that it contains the whole task wrench space:

$$Q(G) = \frac{1}{k_m} \quad (4)$$

$$k_m(G) = \min(k) | T_{ball} \in k \cdot W(G), \quad (5)$$

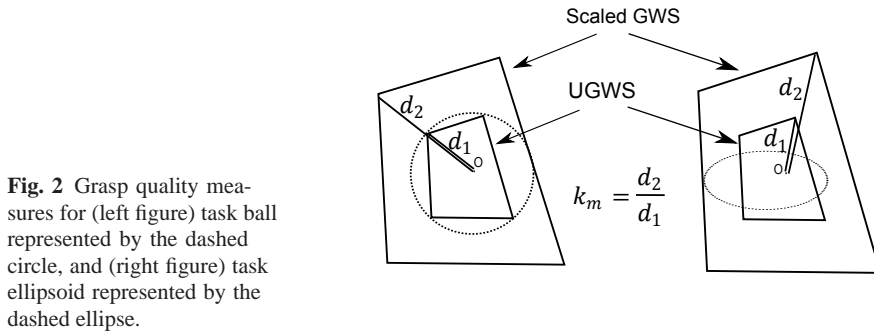


Fig. 2 Grasp quality measures for (left figure) task ball represented by the dashed circle, and (right figure) task ellipsoid represented by the dashed ellipse.

In other words, the $k_m(G)$ is the minimum magnitude of contact force in order to be capable of resisting all task wrenches. The larger k_m is, the greater effort is needed for a grasp to encounter the task wrench along the weakest direction. The grasp planning is to find the maximum $Q(G)$, the reciprocal of $k_m(G)$.

2.2 Measure of Task Wrench

The quality measure in Equ. 4 can also be used for different task requirements instead of using a uniform ball. Related research has been conducted in [4, 7, 8, 9, 10]. Li and Sastry [7] developed a quality criterion to measure the ability of a grasp to perform a task wrench space using a six-dimensional wrench space ellipsoid to better approximate a task (Right of Figure 2). Although this measure takes task requirement into account, they stated that the data acquisition is difficult, so it is challenging to model the task. As reviewed in the Introduction, while most researchers focus on the problems of defining the task wrench space quality and the measurements of how good a grasp can be fitted into a task wrench space, quite few address this practical problem of how to measure the demonstrated task wrench space. Perhaps the only work that measures task wrench space from demonstration was the one conducted by Aleotti and Caselli [18]. In their work, the demonstrated task wrench space was estimated in simulation by mapping the captured hand posture to virtual reality, where a correspondence problem still exists due to two mappings from reality to virtual reality and demonstrated task wrench space from human demonstration to the robot.

Most of the works ([7, 10, 19]) relied on much experience to estimate the task wrench space by predicting the contact disturbance. Taking tool manipulations such as pen, screwdriver, scoop, fork, toothbrush, etc. for example, the contact disturbance is expected to be applied on the tip of those tools. Then the empirical task-oriented disturbance wrench space is a friction cone applied to the tip. The wrench space is assumed to be uniformly distributed in the space. However, even if the disturbance is applied to the same location of different tools, the disturbance wrench can distribute unevenly over the whole task wrench space. Comparing a writing task

and manipulation of a screwdriver, for instance, although both require the grasp to resist disturbance force applied to the tip, they have different disturbance distribution. As illustrated in Figure 3 the comparison between a pen and a screwdriver, the disturbance distributions of them are different. For the writing task, the main disturbance wrench of a writing task is the force pointed to the upper-left direction, and the torque generated along with the force. Hence, the grasp wrench space should be able to apply the opposite force to resist the disturbance, which is distributed primarily in the right area of the friction cone shown in the figure; whereas the main disturbance wrench of the screwdriver is the normal force to the surface and the rotational friction around the principle axis of the screwdriver. Also, the expected disturbance force of the screwdriver is larger than that of the pen. Therefore, different distributions of wrenches in a task wrench space would result in different preferred grasps.

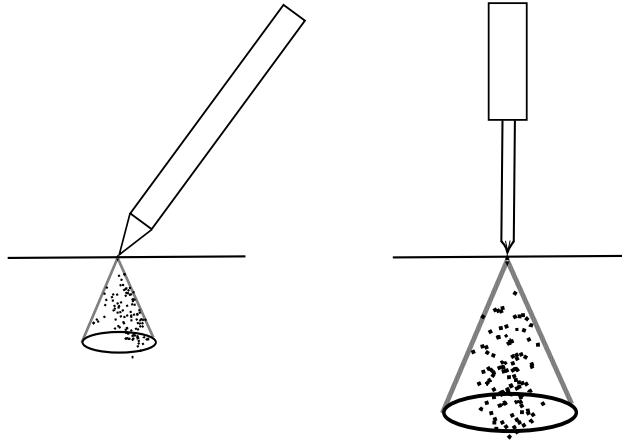


Fig. 3 Disturbance distribution of two tasks. Left figure shows a writing task with a pen; right figure shows a screwing task with a screwdriver.

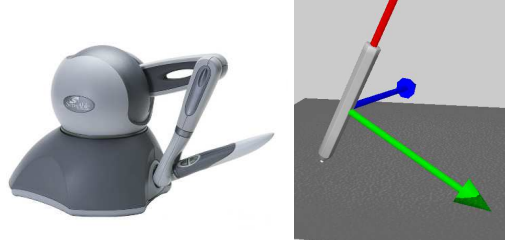
To measure the distribution of the disturbance wrench space, we provided a user interface consisting of a haptic device Phantom Omni, and a virtual reality environment. For each task, a user is asked to manipulate a tool using the haptic device (see Figure 4 for example). The haptic device provides the user with a haptic feedback of the interaction force with the virtual environment. The virtual reality environment was developed based on Chai3D [27], an open source C++ library for computer haptics, visualization, and interactive real-time simulation. It integrates C++ library of Open Dynamic Engine (ODE) for collision detection and OpenGL library for graphical visualization. We integrated the QHull library to calculate the convex Hull [28]. The collision force of the tool is captured in the environment after each iteration. The task wrench space (TWS) is a set of all wrenches measured over time t .

$$TWS = \{w(t) | w(t) = w_c(t) + w_n(t)\} \quad (6)$$

where $w(t)$ is a wrench at time t ; $w_c(t)$ is the contact wrench of the tool with the environment; $w_n(t)$ is non-contact wrench. The non-contact wrench $w_n(t)$ is an offset wrench that includes forces not acting on the surface of the object, such as gravity and other force generated by acceleration. Here, we consider only gravity because motion of the tool is assumed to be pseudo-static. Gravity is considered as the force acting on the center of mass of the object. If the center of mass is set as the torque origin, the wrench compensated by the gravity is a wrench with zero torque. If no contact occurs during the manipulation, only gravity is required to be compensated, e.g., when lifting up a book on an open palm, where the task wrench stabilizes the effect of gravity along a single direction. Note that the direction of the gravity disturbance relative to the object coordinate frame is changing with the motion of the object, e.g., when rotating a book by a hand, where the task wrench stabilizes the effect of gravity along multiple directions.

Since the probability distribution model of disturbance is unknown, for each task, we can build a non-parametric statistical distribution of the disturbance from the dataset of TWS measured by demonstration. Then, to reduce the computational complexity, a smaller set of data points can be randomly sampled based on the non-parametric statistical distribution.

Fig. 4 A user interface for demonstration. Left figure: A haptic device, Phantom OMNI, to manipulate a virtual object. Right figure: the virtual environment.



2.3 Quality Measure Based on Distribution of Task Disturbance

The quality metric k_m in Equ. 4 measures how much effort a grasp needs to cover the whole required task wrench space, which quantifies a constraint in the worst case that the robot should not drop the object. However, the worst case constraint is not always a real guarantee, given that we are modeling the task wrench space from noisy data. Thus, a different quality metric is to be developed that is insensitive to noise.

Furthermore, k_m does not take into account the distribution of a task wrench space. Without considering distribution of a task, it cannot distinguish quality between two task wrenches of the same volume but with different distributions. Consider the scenario of two different GWS for the same TWS shown in Figure 5. It can be observed that the TWS has a higher distribution in the left area. GWS 1 and

GWS 2 in Figure 5a and 5b have the same volume and the same k_m . However, GWS 1 has a higher ability than GWS 1 to apply forces that frequently occur in the task, shown in Figure 5(c).

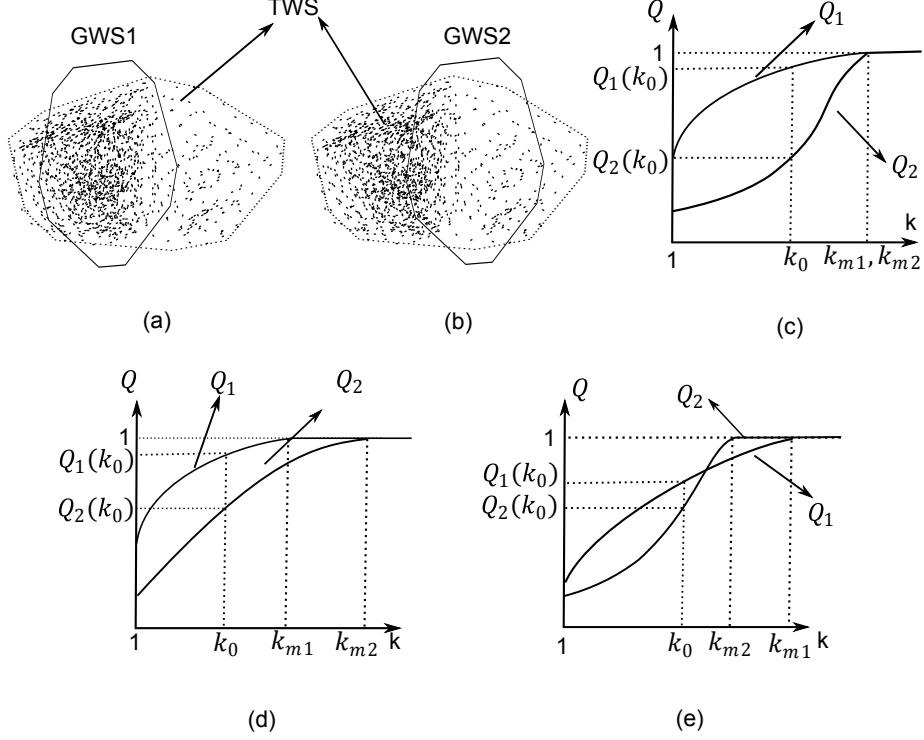


Fig. 5 Comparison of quality measure Q in different scenarios. (a), (b): two grasp wrenches for the same task wrench space; (c): comparison of quality measures Q versus scale k between grasps in (a) and (b). $Q_1(k_0) > Q_2(k_0)$, and $k_{m1} = k_{m2}$; Figures (d) and (e) show the other two cases of Q as a function of scale k : case in (d), $Q_1(k_0) > Q_2(k_0)$, and $k_{m1} < k_{m2}$; case in (e): $Q_1(k_0) > Q_2(k_0)$, and $k_{m1} > k_{m2}$.

Based on the above two reasons, we propose a new task-oriented grasp quality metric that considers both TWS modeled from noisy data, as well as the distribution of TWS. When developing a grasp quality measurement for task-wrench distribution, we must consider the different capabilities along different directions to apply forces. It is preferred that less effort is required of a grasp to apply forces along directions where the disturbance force frequently happens, considering the efficiency of power consumption. The GWS is not necessary to cover the whole TWS, because less capability is required to apply forces for some force directions where force magnitude is large but rarely occurs. Then some noisy outliers may be excluded from the GWS. Intuitively, the grasp quality can be defined as the ratio of TWS that can

be covered by the scaled GWS $W(G)$, given a scale k . The set of task wrenches that is in the scaled GWS is represented as:

$$W = \{w(t) | w(t) \in TWS \cap w(t) \in k \cdot W(G)\} \quad (7)$$

The grasp quality can be represented as:

$$Q(G) = \frac{|W|}{|TWS|} \quad (8)$$

where $|W|$ is the size of the task wrenches covered by the scaled GWS, and $|TWS|$ is the size of total task wrenches; $0 \leq Q(G) \leq 1$. The larger $Q(G)$ is, the more disturbance wrenches can be resisted by the grasp G . Therefore, the grasp planning is to find the optimal grasp that maximizes $Q(G)$.

It is noted that as k increases, Q is not linearly increasing with k , and the increasing rate of Q is not the same for different grasps (Figure 5(c)-(e)). Therefore, the choice of k affects the result of the optimal grasp. Figure 5(c) compares quality Q_1 and Q_2 of the two grasps G_1 and G_2 shown in Figure 5(a) and Figure 5(b) as a function of k . It can be seen that Q_1 increases faster at the beginning. As k becomes larger, the increasing of Q_1 is slowed down. For all $k < k_m$, $Q_1 > Q_2$. when $k \geq k_m$, $Q_1 = Q_2 = 1$. It is also possible that different Q can intersect at some $k < k_m$, as illustrated in Figure 5(e). Also, if choosing a very large value of k , Q of different G is equal to 1. Therefore, it is important to choose a reasonable k that results in a desired Q .

Scale k stands for the amount of force the robotic hand is expected to apply. We suggested a scale k_0 by considering both the capability of the robotic hand, as well as task requirement. Suppose a unit vector \hat{w} stands for a fixed direction for the disturbance wrench $w(t)$. Let $a(t) = \|w(t)\|$, the magnitude of $w(t)$, so that the disturbance wrench can be written as $w(t) = a(t)\hat{w}$. For a given task wrench set, k_0 is determined by the smaller value between the maximum magnitude $a(t)$ of all wrenches in the task, and the maximum forces that can be applied by the robotic hand – typically the capability ω_{max} of robot motors, written as:

$$k_0 = \min(\max(a(t)), \omega_{max}) \quad (9)$$

for all $t = 1, \dots, T$, where T is the number of data samples. In this paper, we used a Barrett hand for the experiment. The maximum finger force of the Barrett hand is $20N$, so we set $\omega_{max} = 20$ in order to bound k_0 . k_0 can also be set to other empirical value, e.g. the amount of force that humans usually apply in a manipulation.

2.4 Incorporation of Thumb Placement Constraint into Grasp Planning

Since a number of anthropomorphic hands have a high number of degrees of freedom (DOF) in order to be as dexterous as human hand, introducing complexity to the search in the optimization, much work has focused on providing constraints to the search space in order to reduce the computational complexity of the search in high dimensional robotic hand configuration space, for example, imposing appropriate contact points on the object (e.g. [20, 21, 22, 23, 24]). The constraint on contact points, however, is assumed to be independent of physical constraints of a given hand. It raises the problem of solving the inverse kinematics that satisfies the constraints imposed by contact points [25]. In this paper, therefore, to avoid the problem given rise by the constraints of contact points, the candidate grasp is computed from a set of given thumb placement on the object surface, as well as the direction thumb should point to. Thumb positions offer a general reference of the body part to be gripped; thumb direction provides a constraint on wrist positions and orientations. The constraint of thumb placement can be labeled manually on the object, or generated automatically from examples.

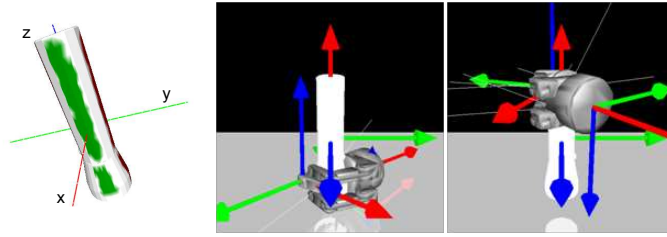


Fig. 6 Illustration of searching procedure constrained by the thumb place and direction. The colored area in the first figure is the area where the thumb is allowed to be placed. Thumb placement in red-colored area can only be pointed to axis x, while thumb placement in green-colored area can only be pointed to axis y.

The upper-left of Figure 6 shows an example of labeled area. The thumb can be placed only on the colored area, with different colors specifying different thumb directions. Thumb placement in the red-colored area can be pointed only to axis x, while thumb placement in green-colored area can be pointed only to axis y. Thumb pose together provide partial constraints to wrist positions/orientations; hence, they reduce the search space during the optimization procedure. Moreover, since the thumb position of the robot is directly translated from the thumb position of the human demonstrator, no mapping between the two very different kinematic systems is required, which avoids the complicated correspondence problem. The user can also specify a grasp type, such as power grasp and precision grasp [29], to better satisfy the task requirement. Figure 6 shows snapshots of a searching procedure of a power grasp throughout the constraint area of thumb placement.

3 Results

In the experiment, we tested our approach for several tasks with different objects. Non-expert subjects were asked to manipulate an object in the user interface via Phantom OMNI. The interaction force between the object and the environment was captured during the demonstration with a sample rate of 100 Hz. The data set of the disturbance, compensated by object gravity, was recorded. Then, from the data set, a non-parametric statistical distribution of the disturbance was built. To reduce the computational complexity, a smaller set of data points was randomly sampled based on the non-parametric statistical distribution.

A Barrett hand model and a Shadow hand model were tested during the simulation for task-oriented grasp planning. The desired grasp type and the constraint area of the thumb location and direction were input into the simulator as well, which highly reduce the search space of the robotic hand configuration. In the simulation, we set the friction coefficient μ to be 1. The friction cone is approximated by an eight-sided pyramid. For each hand configuration, the grasp wrench space can be computed from the contact points and contact normals can be obtained by the open dynamics library. Grasp quality Q was calculated based on the grasp wrench space and the distribution of disturbance. The grasp planning searches the best grasp configuration that maximizes Q .

Figure 7 to Figure 9 show three examples of object manipulation. In the first example, the user was asked to perform a writing motion with a pencil, where the pencil interacts with the environment at the tip. The chosen grasp should be excellent for balancing the pressure and friction at the tip. As shown in Figure 7(a)-(c) the distribution of task wrenches, task wrenches are biased to the positive directions of F_y and F_z , other than the full space of the friction cone. The resulting grasp is, therefore, close to the tip. For the hand configuration shown in Figure 7(d), $Q = 0.8459$ at $k = 2.6$, meaning it covers 84.59% of task wrenches, which is much larger than that of Figure 7(e) where $Q = 0.1968$ at the same k , because it is better to apply force along the F_y and F_z directions than that in Figure 7(e). The quality measures Q_1 and Q_2 changing with scale k for the two grasps are compared in Figure 7(f).

In the second experiment, grasps for two tasks were compared for a knife. The user was asked to perform two tasks: a cutting motion along one direction (+x marked by red color in Figure 8); and a butter spreading motion using both sides of the blade. The disturbance distributions for the two tasks are reported in Figure 8(a)-(d). As shown the cutting task in Figure 8(a), a grasp should be able to generate pressure along -z direction and friction mainly along +x direction to the blade. Torque generated along with the force is shown in Figure 8(b). While for the butter spreading task shown in Figure 8(c) and (d), the task wrenches cover partial area of two opposite friction cone, i.e. the grasp should be able to apply pressure along both +y and -y, and friction along +z. The thumb placement is constraint to the handle. Figure 8(e)-(g) contains evaluations of three grasps for the two tasks respectively (Q_1 for cutting task and Q_2 butter spreading task). For cutting task, where scale k is set to be 8.04, larger than $k = 3.25$ for butter spreading task. It can be seen that for cutting task, the hand configuration in Figure 8(e) is better to apply force in -Fz,

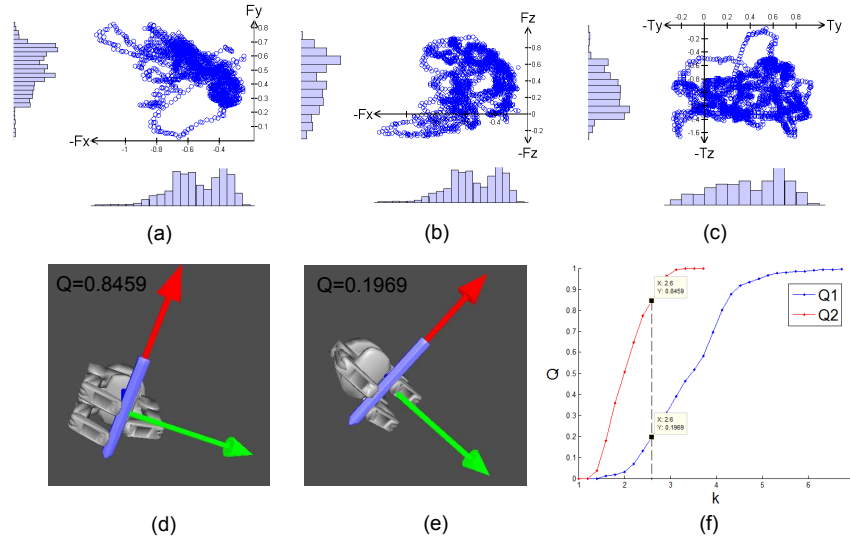


Fig. 7 Planning results for a writing task with a pencil. The center of mass is set to be the origin of the coordinate frame, where axes x , y and z are marked by red, green and blue colors (shown in Figure (d)). (a)-(c): distribution of task wrench projected to F_x - F_y , F_x - F_z , T_y - T_z subspace, respectively, where the task wrench is distributed mainly along $-F_x$, F_y and F_z directions; torque T_z is small so it is not reported here. (d)-(e): two different hand configurations; (f) Grasp quality Q versus scale k for the two hand configurations (Q1 and Q2 are quality measures for hand configuration in (d) and (e)).

along with $-T_y$. The hand configuration in Figure 8(g) has the worst quality measure of the three due to its deficient ability to apply force along z directions; Whereas for the butter spreading task, hand configuration in Figure 8(g) is the best, and Figure 8(e) is the worst.

In the third task, the user was asked to strike a plane with a hammer, and the grasp planning was performed to compare results of the Barrett hand model and the Shadow hand model. It can be imagined that the chosen grasp should be excellent for balancing the large pressure on the head of the hammer. As shown in Figure 9(a)-(b), the distribution covers almost the whole space of the friction cone, whose axis is along $+z$ direction, and the pressure between the hammer and the environment along $+z$ direction is as large as $20N$. The designated grasp type during grasp planning is a power grasp in order to perform powerful manipulation; the scale k of grasp wrench space is set to be 20 for the computation of quality measure. Figure 9 show the results of searching through the feasible area of thumb placement for the Barrett hand model (Figure 9 (c)-(g)), and for the Shadow hand model (Figure 9(h)-(k)). It can be seen that the grasp closer to the head is better to counterbalance the forces that occur at the head. Note that the result of a hammer grasp is different from the intuitive grasping style of humans, who prefer to hold the handle on the other side away from the head, because humans desire to reach a large swing motion with a relatively small arm motion but to generate a large impact force. The grasp

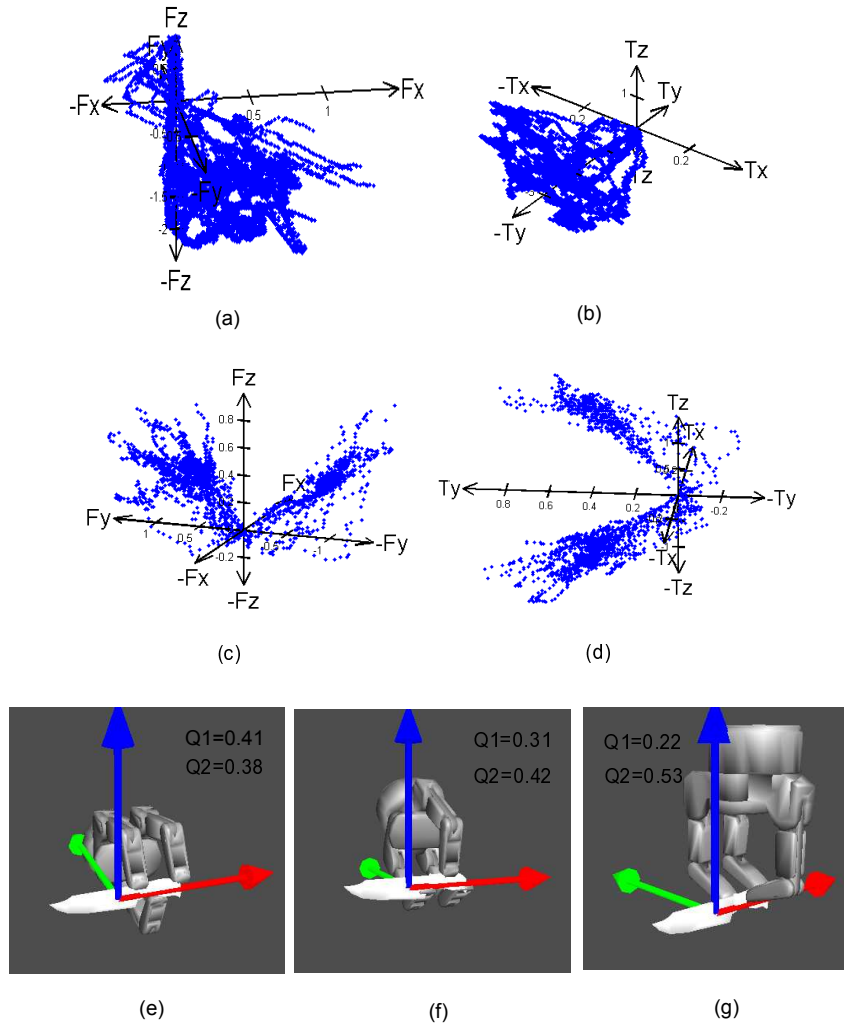


Fig. 8 Planning results for a cutting task and a butter spreading task with a knife. (a)-(b): cutting task distribution of task wrenches projected to F_x - F_y - F_z and T_x - T_y - T_z subspaces respectively, where the task wrenches are distributed mainly in $-F_z$ and F_x ; (c)-(d): the corresponding task wrench distribution for butter spreading task, where the task wrenches are distributed primarily in $+F_y$, $-F_y$, $+F_z$, $+T_z$, $-T_z$; (e)-(g): three different hand configurations. Q_1 is quality measure for the first task, and Q_2 is the quality measure for the second task. Scale k is set to be 8.04 and 3.25 of the two tasks for a precision grasp planning.

optimization considers only the ability to apply force other than the arm and wrist motions. It can be observed from the figure that similar results were obtained for the two hand models, because task distribution and thumb constraint are independent of hand mechanical structures.

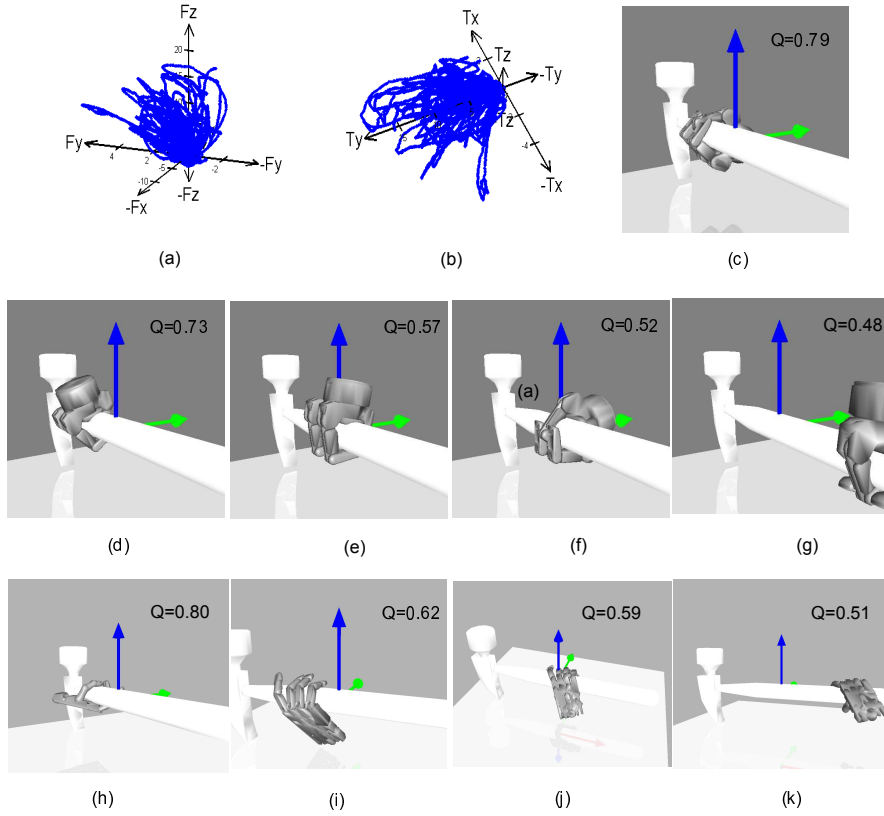


Fig. 9 Planning results for a hammer, where a power grasp is searched because a large power is needed. (a)-(b): distribution of task wrenches projected to $F_x-F_y-F_z$ and $T_x-T_y-T_z$ subspace, respectively, where the task wrenches are distributed mainly in F_z and T_y ; (c)-(g): five different hand configurations of the Barrett hand model; (h)-(k): four different hand configurations of the Barrett hand model. Scale k is set to be 20.

Concluded from the experiments, the resulting grasp with a higher grasp quality criterion tends to be more efficient to apply frequently-occurring force, using the same magnitude of resultant force as the low quality grasp, thus improving the efficiency of power consumption.

4 Conclusion

For task-oriented grasp planning, manipulation tasks are known to be difficult to model. In this paper, a manipulation task was modeled by building non-parametric statistical distribution of disturbance from demonstration data. Instead of an evenly-distributed task wrench space, it is possible that disturbance wrenches in some di-

reactions occur more frequently than the other areas, even if they may be smaller than wrenches that occur less frequently. In favor of grasps that are able to apply frequently-occurring forces, this paper proposes a task-oriented grasp quality criterion based on the distribution of the task disturbance by computing the ratio of disturbance a grasp covers.

To reduce the computational complexity of the search in high-dimensional robotic hand configuration space, as well as to avoid a correspondence problem, the candidate grasp is computed from a set of given thumb placement and thumb direction. The experiment has been validated in simulation with a Barrett hand and a Shadow hand. Both the task model and the demonstration are independent of hand models, so they can be used for other robotic hands.

The hammer example in simulation implies that the resulting robotic grasps may be different from intuitive grasps of the humans, who consider a combination of hand and arm motion as well as force required by a task. Therefore, including arm and hand motion factors in a grasp planning can be a direction of future work.

Another potential improvement is to measure task wrenches on the real object. Then demonstration can be performed on real objects rather than in simulation, so that the user can have more straightforward haptic feeling from the environment. In addition, the TWS can also be updated during the robot execution, which iteratively improves the grasp planning.

Although the current evaluation was conducted in simulation, where a simplified hard contact friction model was defined, the proposed task-oriented grasp quality metric can be extended to other friction models. In the future work, further evaluations will be carried out on real objects and robot platforms.

References

1. Y. Lin, S. Ren, M. Clevenger, and Y. Sun. Learning grasping force from demonstration. In *IEEE International Conference on Robotics and Automation*, pages 1526–1531. IEEE, 2012.
2. D. Kirkpatrick, B. Mishra, and C. K. Yap. Quantitative steinitz's theorems with applications to multifingered grasping. *Discrete & Computational Geometry*, 7(1):295–318, 1992.
3. C. Ferrari and J. Canny. Planning optimal grasps. In *IEEE International Conference on Robotics and Automation*, volume 3, pages 2290–2295, May 1992.
4. N. S. Pollard. Parallel methods for synthesizing whole-hand grasps from generalized prototypes. *Ph.D Dissertation*, 1994.
5. A. T. Miller, S. Knoop, H. I. Christensen, and P. K. Allen. Automatic grasp planning using shape primitives. In *IEEE International Conference on Robotics and Automation*, volume 2, pages 1824–1829, Sep 2003.
6. K. Hsiao, M. Ciocarlie, P. Brook, and W. Garage. Bayesian grasp planning. In *ICRA Workshop on Mobile Manipulation: Integrating Perception and Manipulation*, 2011.
7. Z. Li and S. S. Sastry. Task-oriented optimal grasping by multifingered robot hands. *IEEE Journal of Robotics and Automation*, 4(1):32–44, feb 1988.
8. L. Han, J. C. Trinkle, and Z. X. Li. Grasp analysis as linear matrix inequality problems. *IEEE Transactions on Robotics and Automation*, 16(6):663–674, 2000.
9. C. Borst, M. Fischer, and G. Hirzinger. Grasp planning: how to choose a suitable task wrench space. In *IEEE International Conference on Robotics and Automation*, volume 1, pages 319–325, May 2004.

10. R. Haschke, J. J. Steil, I. Steuwer, and H. Ritter. Task-oriented quality measures for dextrous grasping. In *IEEE International Symposium on Computational Intelligence in Robotics and Automation*, pages 689–694, June 2005.
11. A. Sahbani, S. El-Khoury, and P. Bidaud. An overview of 3d object grasp synthesis algorithms. *Robotics and Autonomous Systems*, 60(3):326–336, 2012.
12. S. Ren and Y. Sun. Human-object-object-interaction affordance. In *IEEE Workshop in Robot*, pages 1–6. IEEE, 2013.
13. Y. Sun, S. Ren, and Y. Lin. Human-object-object-interaction affordance. In *Robotics and Autonomous System*, pages 1–10, In Press.
14. Y. Lin and Y. Sun. Grasp mapping using locality preserving projections and knn regression. In *International Conference on Robotics and Automation*, volume 3, May 2013.
15. A. Billard, S. Calinon, R. Dillmann, and S. Schaal. Robot programming by demonstration. In *Handbook of Robotics*. MIT Press, 2008.
16. J. Romero, H. Kjellstrm, and D. Kragic. Human-to-robot mapping of grasps. In *IEEE/RSJ International Conference on Intelligent Robots and Systems, WS on Grasp and Task Learning by Imitation*, 2008.
17. M. Hueser and J. Zhang. Visual and contact-free imitation learning of demonstrated grasping skills with adaptive environment modelling. In *IEEE/RSJ International Conference on Intelligent Robots and Systems, WS on Grasp and Task Learning by Imitation*, 2008.
18. J. Aleotti and S. Caselli. Interactive teaching of task-oriented robot grasps. *Robotics and Autonomous Systems*, 58(5):539–550, 2010.
19. N. S. Pollard. Closure and quality equivalence for efficient synthesis of grasps from examples. *The International Journal of Robotics Research*, 23(6):595–613, 2004.
20. V. D. Nguyen. Constructing force-closure grasps. *The International Journal of Robotics Research*, 7(3):3–16, 1988.
21. J. Ponce and B. Faverjon. On computing three-finger force-closure grasps of polygonal objects. *IEEE Transactions on Robotics and Automation*, 11(6):868–881, 1995.
22. X. Zhu and J. Wang. Synthesis of force-closure grasps on 3-d objects based on the q distance. *IEEE Transactions on Robotics and Automation*, 19(4):669–679, 2003.
23. J. Liu, G. Xu, X. Wang, and Z. Li. On quality functions for grasp synthesis, fixture planning, and coordinated manipulation. *IEEE Transactions on Automation Science and Engineering*, 1(2):146–162, 2004.
24. M. A. Roa and R. Suárez. Finding locally optimum force-closure grasps. *Robotics and Computer-Integrated Manufacturing*, 25(3):536–544, 2009.
25. C. Rosales, L. Ros, J. M. Porta, and R. Suárez. Synthesizing grasp configurations with specified contact regions. *The International Journal of Robotics Research*, 30(4):431–443, 2011.
26. D. Prattichizzo and J. C. Trinkle. Grasping. *Springer Handbook of Robotics*, pages 671–700, 2008.
27. F. Conti, D. Morris, F. Barbagli, and C. Sewell. Chai 3d. Online: <http://www.chai3d.org>, 2006.
28. C. B. Barber and H. Huhdanpaa. Qhull. *The Geometry Center, University of Minnesota*, <http://www.geom.umn.edu/software/qhull>, 1995.
29. W. Dai, Y. Sun, and X. Qian. Functional analysis of grasping motion. In *IEEE/RSJ International Conference on Intelligent Robots and Systems*, 2013.